Neuroendocrinology Letters Volume 43 No. 2 2022
ISSN: 0172-780X; ISSN-L: 0172-780X; Electronic/Online ISSN: 2354-4716
Web of Knowledge / Web of Science: Neuroendocrinol Lett
Pub Med / Medline: Neuro Endocrinol Lett

ORIGINAL ARTICLE

Changes in vesicular glutamate transporter 2 (Vglut2) and vesicular GABA transporter 1 (Vgat1) in the orofacial pain and temperature perception pathway under low estrogen conditions

Jinglin Zhang[1], Yunmeng Da[2], Jiali Lu[1], Yanrong Sun[3], Hanfei Wang[3], Ke Wang[3], Wenjuan Wang[3], Lihua Qin[3], Jing Jia[1,4]

1 Shanxi Medical University School and Hospital of Stomatology,Taiyuan, China.
2 Hebei Provincial Key Laboratory of Ophthalmology, Hebei Clinical Medical Research Center of Eye Diseases, Department of Prosthodontics, Hebei Eye Hosipital, Quanbei East Street, No.399, Xiangdu, Xingtai, China.
3 Department of Anatomy, Histology and Embryology School of Basic Medical Sciences, Peking University Health Science Center, Beijing, China.
4 Department of Stomatology, The Third Medical Center, Chinese PLA (People's Liberation Army) General Hospital, Beijing, China.

Correspondence to: **Jing Jia**
Department of Stomatology,The Third Medical Center, Chinese PLA (People's Liberation Army) General Hospital, Beijing 100039
tel: +86-13611266262, e-mail: jiajing1996@aliyun.com
Lihua Qin
Department of Anatomy, Histology and Embryology, School of Basic Medical Science, Peking University Health Science Center. Beijing, 100191, China
tel: +86-010-82801427, e-mail: qinlihua88@163.com

Submitted: 2022-05-26 Accepted: 2022-06-30 Published online: 2022-06-30

Key words: **Perimenopause; Orofacial discomfort; Estrogen; glutamatergic neurons; GABAergic neurons**

Neuroendocrinol Lett 2022; **43**(2):88–98 **PMID:** 35933616 NEL430222A07 © 2022 Neuroendocrinology Letters • **www.nel.edu**

Abstract

OBJECTIVE: To investigate the effects of estrogen on the threshold and temperature of orofacial pain and explore the influence on the function of glutamate and GABA neurons in the orofacial pain temperature perception pathway by observing the expression of vesicular glutamate transporter 2 (Vglut2) and vesicular GABA transporter 1 (Vgat1).

METHODS: A total of 24 adult female Sprague–Dawley rats were divided into three groups: sham operation (SHAM), ovariectomized (OVX) and ovariectomized plus estrogen intervention (OVX+E) (n = 8 per group). The threshold of mechanical pain of the orofacial region was assessed with von Frey filaments, and the temperature of the rat orofacial region was monitored by infrared thermography. Changes in the expression of Vglut2 and Vgat1 in glutamatergic and GABAergic neurons in the trigeminal ganglion (TG), spinal trigeminal nucleus (Sp5C), lateral parabrachial nucleus (LPB) and ventral posteromedial nucleus of the thalamus (VPM) were assessed by immunostaining and Western blotting.

RESULTS: Under low-estrogen conditions, the mechanical pain threshold of the orofacial region of rats decreased significantly, and the temperature of the orofacial region increased significantly. The expression of Vglut2 and Vgat1 in the TG and Sp5C showed a downward trend, and the decline in Vgat1 was greater than

that in Vglut2. Conversely, both proteins were upregulated in the LPB and VPM, and the magnitude of the changes in Vglut2 was greater than that in Vgat1. Estrogen therapy reversed these changes.

CONCLUSION: Under low-estrogen conditions, the proportion of glutamate and GABA neurons in the orofacial pain and temperature sensation pathway changes, which leads to the imbalance of neurotransmission function and the enhancement of excitatory transmission of these two kinds of neurons and finally leads to a decrease in the orofacial pain threshold and an increase in temperature.

INTRODUCTION

The decline in ovarian function in perimenopausal women leads to a decrease in the level of estrogen, during which all systems of the body are affected, such as decreased saliva secretion and burning mouth syndrome (Meurman *et al.* 2009; Monteleone *et al.* 2018; Song *et al.* 2019). Epidemiological surveys show that approximately 90% of women with burning mouth syndrome are postmenopausal (Kim *et al.* 2014). Patients with burning mouth syndrome often complain of tongue pain, oral mucous membrane burning pain, some accompanied by headache, sore throat, neck and esophageal pain (Ritchie & Kramer,2018). However, the mechanism of occurrence is not clear. Studies have found that lingual nerve block anesthesia can relieve the burning sensation in patients with burning mouth syndrome, suggesting that burning sensation may be related to the dysfunction of the pain conduction pathway (Jääskeläinen & Woda, 2017). In the classical orofacial pain and temperature perception pathway, receptors, such as those in the orofacial skin and mucosa, receive a variety of nociceptive signals, which are transmitted to the TG through its peripheral processes. These signals are projected to the Sp5C and then divided into two parts, one to tertiary neurons in the VPM and the other part to the LPB. Finally, the integrated signals are received by the cerebral cortex (Shinoda *et al.* 2019; Bičanić *et al.* 2019).

The orofacial sensory signal transduction pathway consists of excitatory glutamatergic neurons and inhibitory GABAergic neurons, which are in equilibrium under physiological conditions. When GABAergic neurons are insufficient to inhibit glutamatergic neurons, sensory signals continue to be transmitted in an excitatory manner, resulting in pain. In contrast, sensory signal transduction is suppressed and does not produce pain. If the balance between glutamate and GABA neurons is disrupted, it might lead to abnormal transmission of pain (Kuner, 2010).

It has been found that local application of a glutamate receptor antagonist to the spinal trigeminal nucleus can also antagonize the increase in neuronal activity caused by orofacial temporomandibular joint disease (Tashiro *et al.* 2015). However, injection of a GABA receptor agonist into the TG can attenuate the activity in the spinal trigeminal nucleus induced by electrical stimulation of the masseter muscle in rats (Ranjbar & Cairns, 2021). Other scholars have found that after orofacial trigeminal nerve injury, an increase in the number of glutamatergic synaptic contours and a decrease in average synaptic length in the spinal trigeminal nucleus may lead to the activation of nociceptive pathways, thus promoting the development of orofacial pain (Laursen *et al.* 2014). In addition, specific activation of glutamatergic neurons in the LPB or specific inhibition of GABAergic neurons can both induce pain responses in the mouths and faces of mice (Wang & Xu, 2021). Subsequently, it is believed that the balance between glutamatergic and GABAergic neurons is the key to the normal and orderly transmission of orofacial sensory information.

At present, the effect of estrogen on pain transduction is not clear. Some scholars believe that estrogen can promote pain, while other studies elucidate that estrogen has an inhibitory effect on pain (Yu *et al.* 2011; Reddy *et al.* 2021; Zhang *et al.* 2021). It has been reported that in vitro cell experiments the membrane receptor of estrogen can lead to the loss of the function of GABA neurons, weaken inhibitory transmission and promote the pain effect (Luo *et al.* 2016). Studies on dorsal root ganglion showed that estrogen interacts with mGluR2/3, a metabolic glutamate receptor, through its receptor ER α, which rapidly inhibits calcium influx mediated by estradiol and inhibits nociceptive information transmission and thus inhibits the production of pain (Micevych & Mermelstein. 2008). In addition, it was found that estradiol can induce the mRNA expression of glutamate decarboxylase in the hippocampus, which is the key enzyme to convert glutamate to GABA, so that more glutamate is converted to GABA, enhancing the function of GABAergic neurons and playing a role in inhibiting pain (Ma *et al.* 2020). Thus, the specific regulatory effect of estrogen on pain is region-specific and related to the type of estrogen receptor. It has been found that estrogen receptors are widely distributed in the temperature sensation pathway of orofacial pain, but the specific effect of estrogen on the transmission of orofacial pain has not been reported (Warfvinge *et al.* 2020).

In glutamatergic neurons, there are three subtypes of vesicular transporters responsible for glutamate release: Vglut1, Vglut2 and Vglut3. Vglut1 and Vglut2 are specifically expressed in glutamatergic neurons and are labeled proteins of glutamatergic neurons. It has been found that neurons projecting from the spinal trigeminal nucleus to the thalamus only express Vglut2 in the orofacial pain and temperature sensation pathway (Herzog *et al.* 2004). Similar to glutamatergic neurons, there are also three subtypes of transporters in GABA neurons: Vgat1, Vgat2 and Vgat3. According to a localization study of these three transporters, Vgat1 is widely expressed in the orofacial sensory information

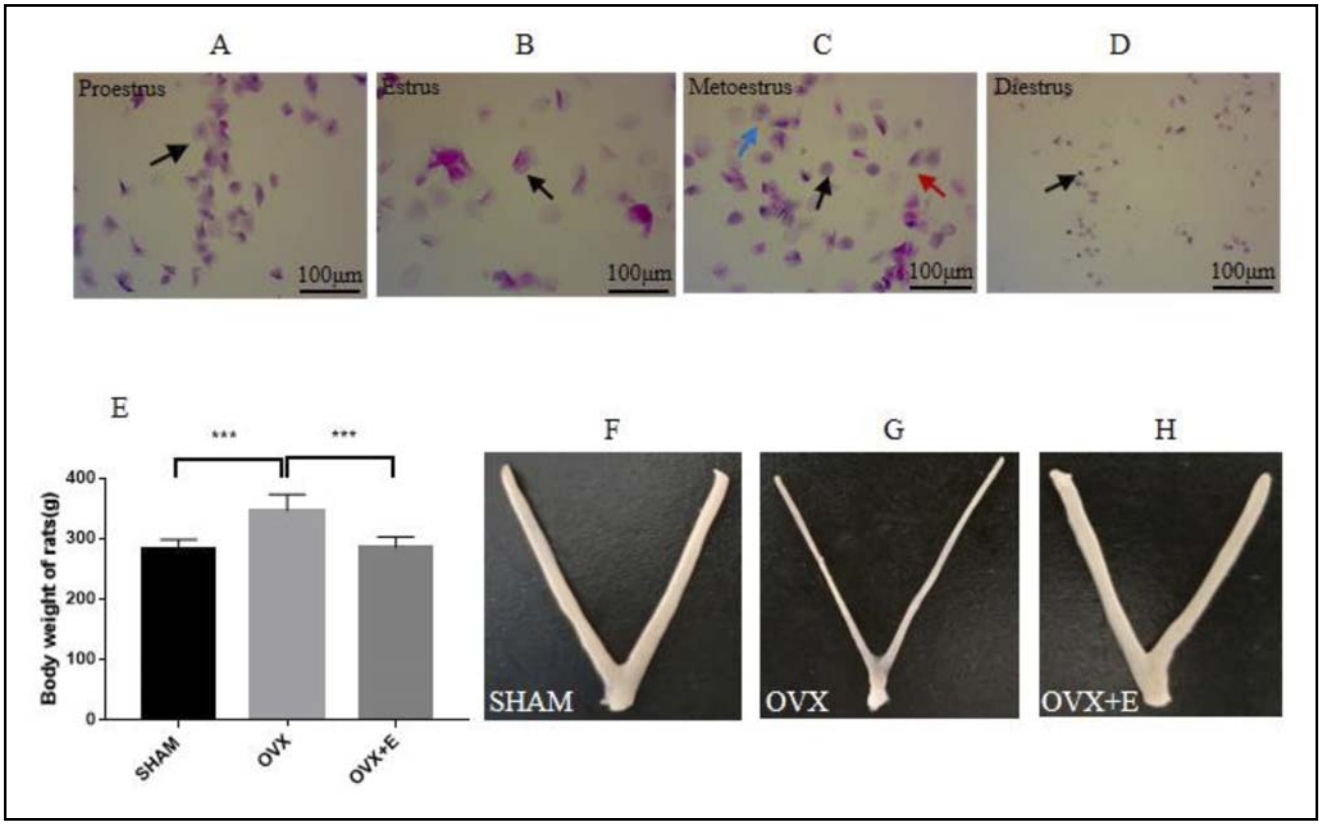

Fig. 1. Validation of successful ovariectomies. (A-D) Proestrus, estrus, metestrus and interestrus, respectively. The arrow represents positive cells, Bar= 100 μm. (E). Body weight of rats in the SHAM , OVX and E2 groups. (F-H) Uterus morphology of the SHAM, OVX and OVX+ groups. Bar=100 μm. The data are represented as the mean ± standard deviation (SD). *$P < 0.05$, **$P < 0.01$, ***$P < 0.001$.

pathway and plays a major role in the GABA system (Sears & Hewett. 2021). Numerous studies have shown that glutamate and GABA neurons are under the regulation of estrogen, which is manifested by mediating the two proteins Vglut2 and Vgat1 (Kiss *et al.* 2013;Hrabovszky *et al.* 2006;Moore *et al.* 2018;Almey *et al.* 2016). Hence, the following questions arise: Will estrogen have a similar effect on the balance of the two types of neurons in the orofacial pain and temperature perception pathway? Are these effects the same for different nuclei in the pathway? We conducted a study to answer these questions.

MATERIALS AND METHODS

Establishment of animal model

Twenty-four female Sprague–Dawley rats aged 6-8 weeks and weighing 225±10 g were obtained from the Animal Experimental Center of Peking University Health Science Center. The rats were housed in an SPF-grade animal facility at a constant temperature of 25±1°C and relative humidity of 40-50% on a 12 h light/dark cycle. All rats were allowed free access to food and water.

Before animal experimentation, the study protocol was approved by the Ethics Committee for Laboratory Animal Welfare. Twenty-four rats were randomly divided into three groups: the sham-operated, ovariectomized (OVX), and estrogen-treated ovariectomized (OVX+E) groups (8 rats in each group). After anesthetization with 40 mg/kg 1% sodium pentobarbital, animals in the sham group underwent laparotomy, but the ovaries were not removed. Animals in the remaining two groups underwent ovariectomy. The rats were weighed weekly during this period to adjust the dose of the drug. Two weeks after the animals in the OVX + E group received daily subcutaneous injections of estrogen (25 μg/kg), the animals in the OVX and SHAM groups were injected with an equal volume of the vehicle (sterile sesame oil) at the same site for six weeks.

Von Frey filaments and orofacial mechanical pain

All rats were placed in clean, nonoccluded cages and allowed to acclimate for at least 30 min before the start of the behavioral experiments. Filaments with bending forces of 1 (0.04 g), 2 (0.07 g), 3 (0.16 g), 4 (0.4 g), 5 (0.6 g), 6 (1.4 g), 7 (4.0 g), and 8 (8.0 g) were applied to the ipsilateral and contralateral whisker pads. Backward movement, flexion or head withdrawal after application of the filament was considered a response. The rat mechanical head withdrawal threshold (g) was calculated as (10[Xf+kδ])/10000, where XF represents the bending force of the last filament applied,

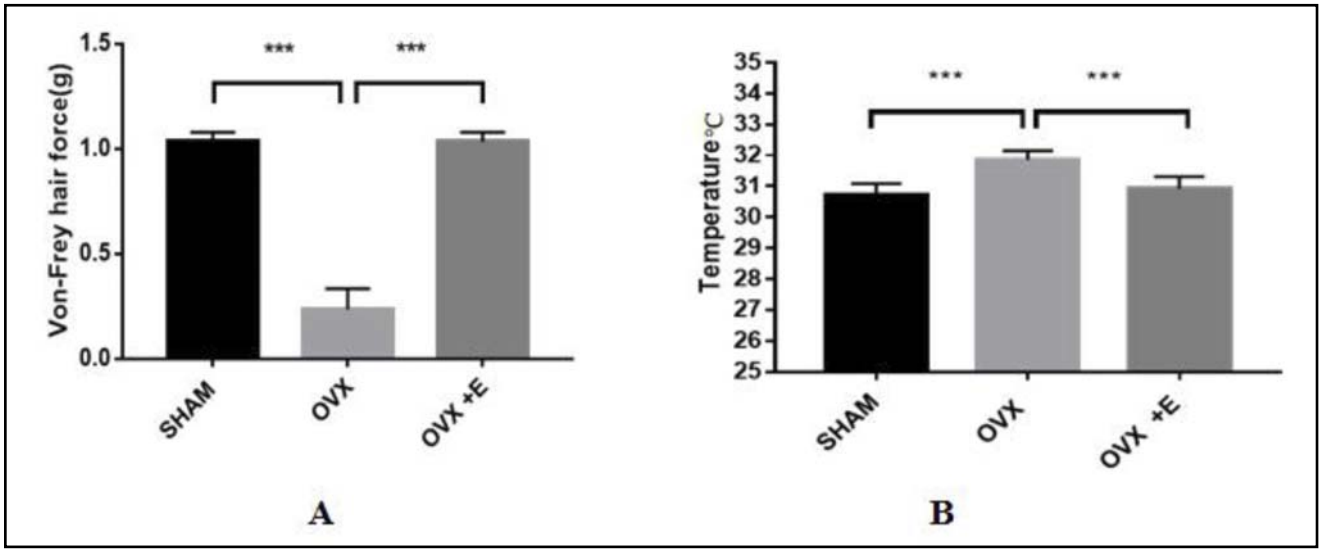

Fig. 2. (A) Changes in the threshold of orofacial mechanical pain in the SHAM, OVX and OVX+E groups. (B) Changes in the orofacial temperature in the SHAM, OVX and OVX+E groups. *P < 0.05, **P < 0.01, ***P < 0.001.

δ represents the mean difference between the bending force of each filament after taking the logarithm (for the filaments selected in this experiment, δ was equal to approximately 0.356), and K is the coefficient value obtained after calculation of the "X" and "O" sequences obtained from infrared measurements.

Thermographic monitoring of rat orofacial temperature

The rats were placed in a quiet environment for 10 min and allowed to adapt to the environment. They were subsequently placed in a lidless container for behavioral assays. Infrared thermography was performed for 10 min, during which the rats were allowed to move freely. The surface temperature of orofacial sites of live rats was randomly captured during the photographing period. The captured images were imported into the analyzer software for subsequent image processing and analysis.

Immunohistochemical staining

Nine rats (three from each group) were randomly selected and perfused intracardially with normal saline (0.9%, 4°C) and paraformaldehyde (4%, 4°C) after anesthesia, and the brains and trigeminal ganglia were obtained. Brain tissue was postfixed in 4% paraformaldehyde for 8~112 h, and the fixed tissue blocks were placed in a 30% sucrose solution at 4°C until they sank to the bottom. The TG was cut into 20-μm-thick sections. The Sp5C, VPM and LPB were identified according to the sixth edition of a rat brain atlas and cut into 20-μm-thick sections. Three sections were randomly selected from each rat for immunohistochemical staining of VGLUT2, and another 3 sections were used for immunohistochemical staining of VGAT. The frozen sections were placed in 0.3% Triton and incubated at 37°C for 40 min. Afterward, they were immersed in boiling sodium citrate for 10 min for antigen retrieval. The sections were then immersed in 3% hydrogen peroxide for 15 min, washed in PBS, incubated with goat serum for 1 h at room temperature, incubated with a mouse anti-VGLUT2 antibody (1:250, Novus, nbp2-59330) or rabbit anti-Vgat1 antibody (1:400, Novus, nbp2-20857) overnight at 4°C, and incubated with biotinylated goat anti-rabbit IgG or biotinylated goat anti-mouse IgG for 2 h at room temperature. After washing with PBS, the sections were incubated with horseradish peroxidase-labeled streptavidin for 3 h at room temperature (Zhongshan Golden Bridge Kit) and developed with 3,3'-diaminobenzidine (DAB) color development solution for 3 min. Panoramic images were acquired with a pathological section scanner (NanoZoomer Digital Pathology system; Hamamatsu, Japan). Two fields of each section were randomly selected, and the optical density and area were analyzed using Image-Pro Plus 6 Software (Media Cybernetics, Inc., Rockville, MD, USA). The average optical density (AOD) was calculated as ΣIOD/Σarea.

Western blotting

Fifteen rats (5 rats from each group) were randomly selected, anesthetized and decapitated. The TG and brain were immediately removed, and a metal rat brain mold was used to identify the VPM in coronal sections according to coordinates obtained from a rat brain atlas: 3.12-3.96 mm anteroposterior to bregma; 1.60-3.80 mm mediolateral from bregma; and 5.10-6.80 mm deep from the dura. The LPB was identified according to the following coordinates: 8.76-9.60 mm anteroposterior to bregma; 1.40-2.80 mm mediolateral from bregma; and 6.40-7.00 mm deep from the dura. The Sp5C area was identified according to the following coordinates: 14.28-15.96 mm anteroposterior to bregma; 1.60-3.40 mm mediolateral from bregma; and 7.20-9.20 mm deep from the dura. The

tissue samples were homogenized in cold lysis buffer containing 1% protease inhibitor by ultrasonication. A BCA assay kit (Applygen Technologies Inc., P1511-1) was used to determine the protein concentration of each sample. The proteins were separated on a 10% sodium dodecyl sulfate-polyacrylamide gel (80 V, 120 min). The proteins were transferred from the gel to a nitrocellulose membrane (Applygen Technologies Inc.) at 100 V. Then, the membrane was shaken slowly on a shaker in blocking buffer (5% bovine serum albumin (BSA) in TBST) at room temperature for 1 h. The membrane was incubated with mouse anti-vglut2, rabbit anti-VGAT, mouse anti-β-actin (Applygen Technologies Inc., C1313) and rabbit anti-GAPDH (Applygen Technologies Inc., C1340) antibodies diluted 1:200, 1:400, 1:3000 and 1:3000, respectively, in TBST containing 5% BSA overnight. The membrane was then incubated with goat anti-mouse (anti-vglut2/β-actin primary antibodies), goat anti-rabbit (anti-VGAT/GAPDH primary antibodies) or goat anti-rabbit (anti-β-actin primary antibody) antibodies in TBST containing 5% BSA at room temperature for 2 h with shaking. For development using ECL reagent, after 2 min, the membrane was placed in a high-sensitivity chemiluminescence imager, and appropriate conditions were selected for exposure. The grayscale values of the bands were analyzed with Image-Pro Plus software.

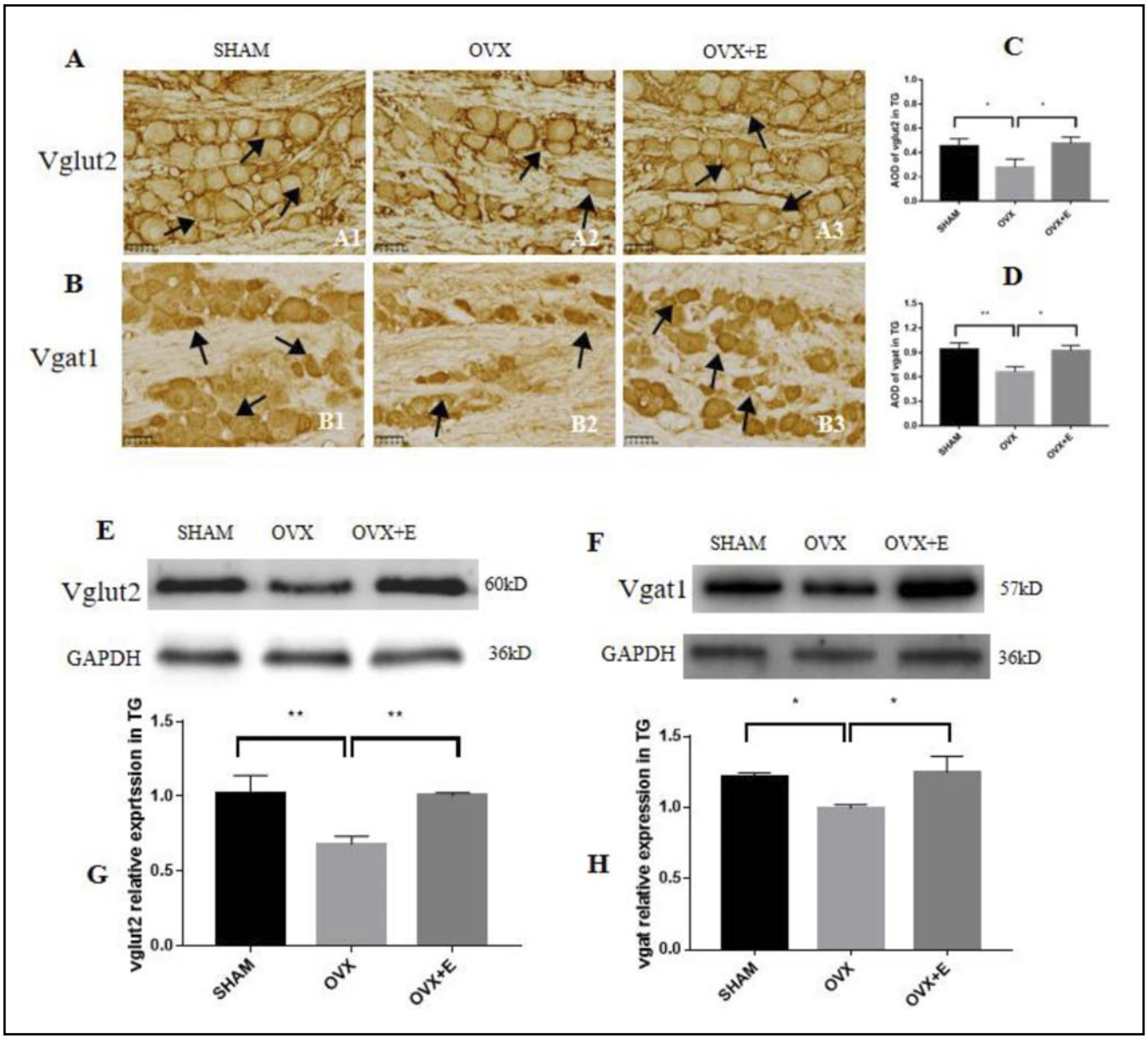

Fig. 3. (A) Immunohistochemical staining of Vglut2 in the TG in the SHAM (A1), OVX (A2) and OVX+E (A3) groups. (C) Analysis of the AOD of Vglut2 in the TG. (B) Immunohistochemical staining of Vgat1 in the TG in the SHAM (B1), OVX (B2) and OVX+E (B3) groups. (D) Analysis of the AOD of Vglut2 in the TG. Bar=50 μm. The arrows indicate Vglut2- and Vgat1-positive cells. (E-H) Western blot analysis of Vglut2 and Vgat1 in the three groups. (E, G) Immunoblots of Vglut2 (60 kD) and GAPDH (36 kD) and relative protein levels (Vglut2/GAPDH) in the TG. (F, H) Immunoblots of Vgat1 (57 kD) and GAPDH (36 kD) and relative protein levels (Vgat1/GAPDH) in the TG. $^{*}P < 0.05$, $^{**}P < 0.01$, $^{***}P < 0.001$.

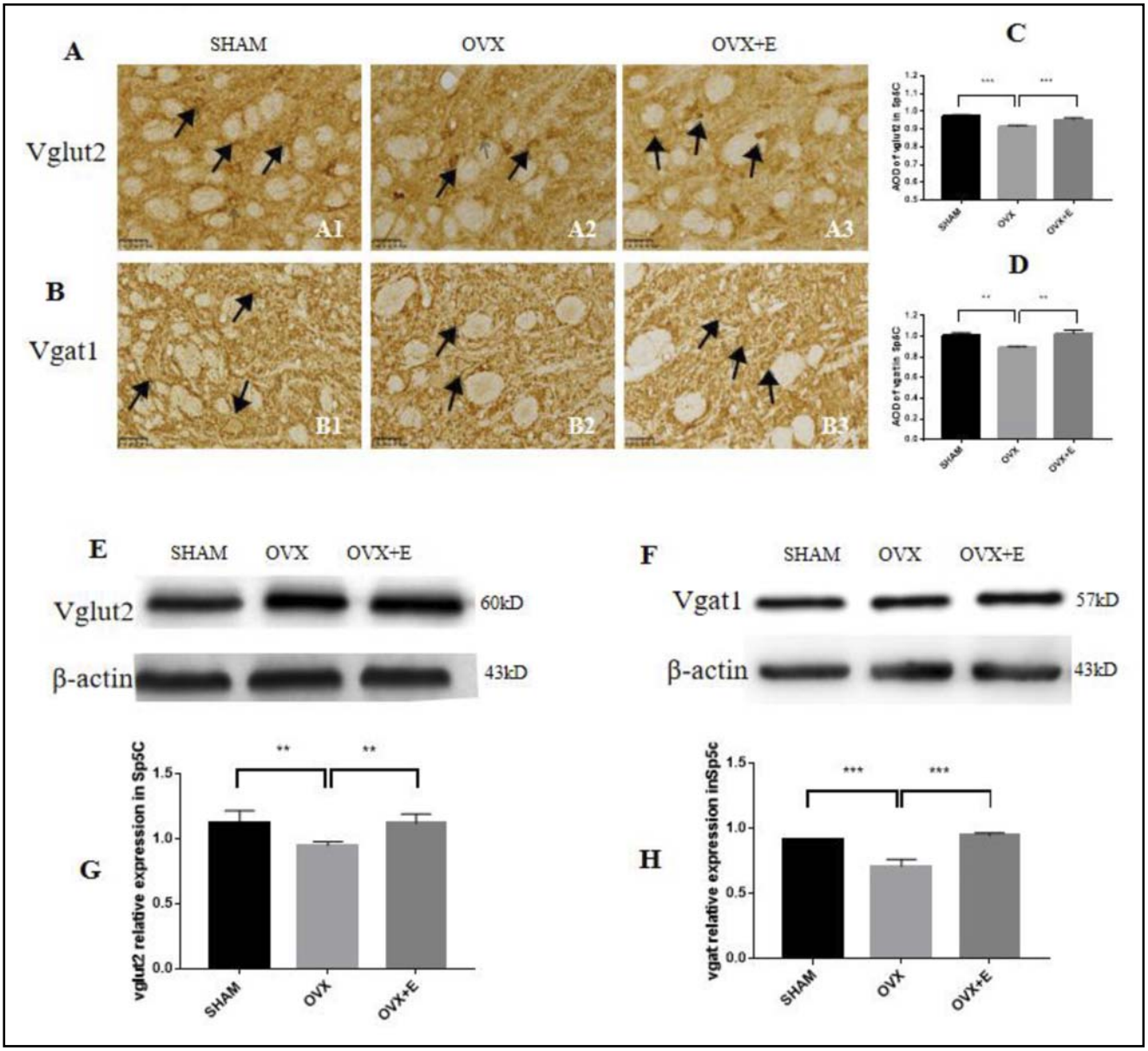

Fig. 4. (A) Immunohistochemical staining of Vglut2 in the Sp5C in SHAM (A1), OVX (A2) and OVX+E (A3) groups. (C) Analysis of the AOD of Vglut2 in the Sp5C. (B) Immunohistochemical staining of Vgat1 in Sp5C in the SHAM (B1), OVX (B2) and OVX+E (B3) groups. (D) Analysis of the AOD of Vgat1 in the Sp5C. Bar=50 μm. The arrows indicate Vglut2- and Vgat1-positive cells. (E, G) Immunoblots of Vglut2 and β-actin (43 kD) and relative protein levels (Vglut2/β-actin) in Sp5C cells. (F, H) Immunoblots of Vgat1 and β-actin and relative protein levels (Vgat1/β-actin) in Sp5C. *$P < 0.05$, **$P < 0.01$, ***$P < 0.001$

Statistical analysis

Data are expressed as the mean±standard deviation and were analyzed using SPSS software. $P<0.05$ indicated statistical significance. All the data were processed using one-way analysis of variance (ANOVA), followed by least squares difference post hoc test. Moreover, a normal distribution test and homogeneity test of variance were both used before ANOVA.

RESULTS

Ovariectomized versus SHAM operated rats

Vaginal exfoliated cell smear staining showed that vaginal exfoliated cells in the SHAM group showed continuous changes in the estrous cycle, mainly polygonal nucleated epithelial cells in proestrus (Fig. 1A) and estrus (Fig. 1B), and leukocytes, keratinized nucleated epithelial cells and polygonal nucleated epithelial cells coexisted in the late stage of estrus (Fig. 1C). The main manifestation of diestrus in the OVX group was single, small and round nucleated cells (Fig. 1D).

The uterine shape of the SHAM group (Fig. 1F) was plump, while that of the OVX group (Fig. 1G) was

significantly thinner. The shape of the uterus recovered obviously in the OVX+E group (Fig. 1H).

The body weight of rats in the OVX group was significantly higher than that in the SHAM and OVX+E groups (OVX: 346.8±8.5 vs. SHAM: 282.6±5.9 g, $P<0.01$). However, there was no significant difference between the SHAM group and OVX+E group (SHAM: 282.6±5.9 vs. OVX+E: 285.7±7.1 g, $P>0.05$). The results are shown in Figure 1E.

Threshold mechanical pain and orofacial temperature

The threshold of orofacial mechanical pain in the OVX group was significantly lower than that in the SHAM and OVX+E groups (OVX: 0.24±0.09 vs. SHAM: 1.03±0.04 g, $P<0.01$). However, there was no significant difference between the SHAM group and OVX+E group (SHAM: 1.03±0.04 vs. OVX+E: 1.03±0.05 g, $P>0.05$). The results are shown in Figure 2A.

The orofacial temperature in the OVX group was significantly higher than that in the SHAM and OVX+E groups (OVX: 31.86±0.03 vs. SHAM: 30.72±0.04°C, $P<0.01$). However, there was no significant difference between the SHAM group and OVX+E group (SHAM: 30.72±0.04 vs. OVX+E: 30.93±0.04°C, $P>0.05$). The results are shown in Figure 2B.

Immunohistochemical staining and Western Blot

Expression of Vglut2 and Vgat1 in TG

Immunohistochemistry showed that Vglut2 (Fig. 3A1-A3) and Vgat1 (Fig. 3B1-B3) were expressed in the TG. The AOD values for Vglut2 and Vgat1 in the OVX

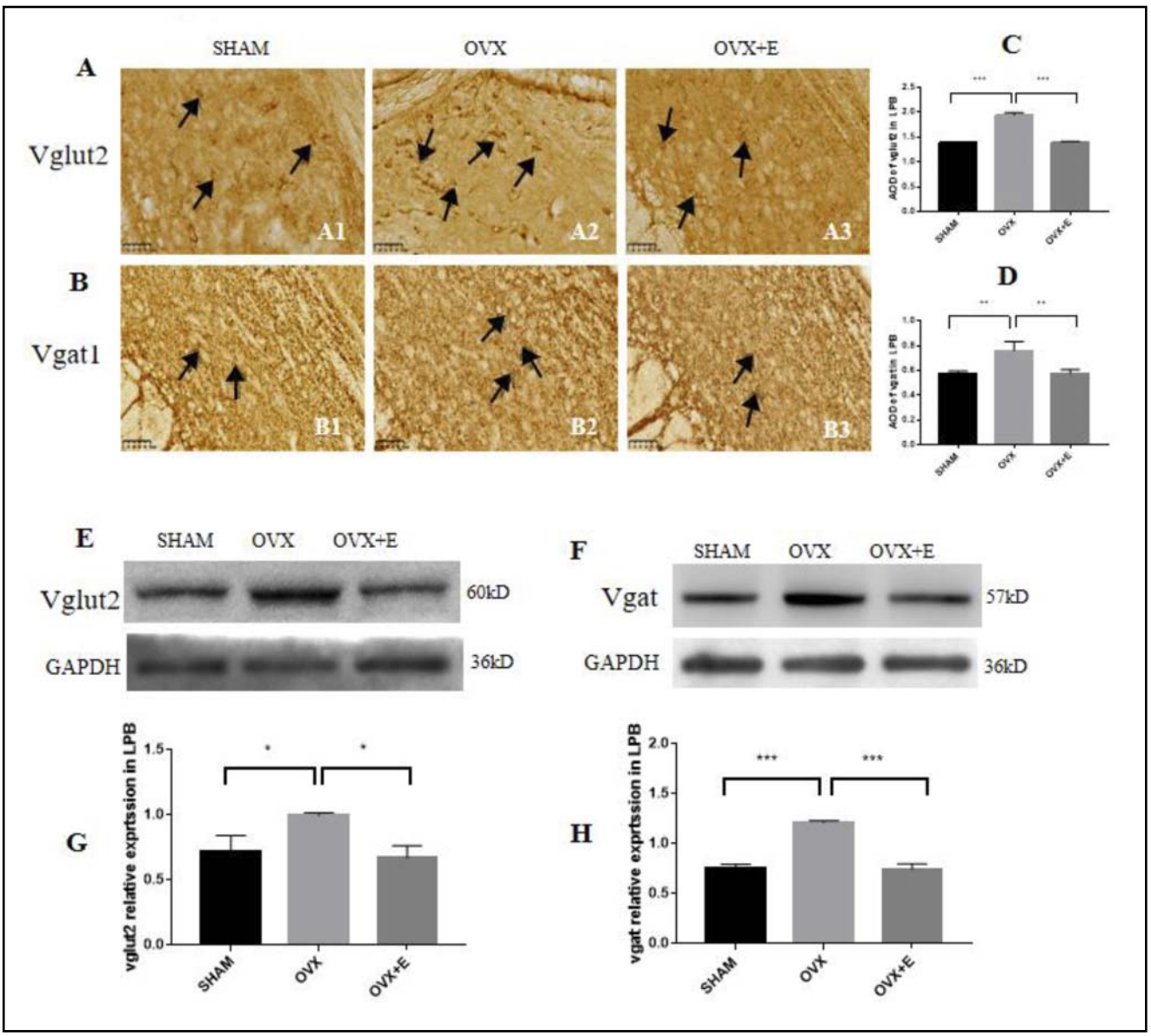

Fig. 5. (A) Immunohistochemical staining of Vglut2 in the LPB in the SHAM (A1), OVX (A2) and OVX+E (A3) groups. (C) Analysis of the AOD of Vglut2 in the LPB. (B) Immunohistochemical staining of Vgat1 in the LPB in the SHAM (B1), OVX (B2) and OVX+E (B3) groups. (D) Analysis of the AOD of Vgat1 in the LPB. Bar=50 μm. The arrows indicate Vglut2- and Vgat1-positive cells. (E, G) Immunoblots of Vglut2 and β-actin and relative protein levels (Vglut2/β-actin) in the LPB. (F, H) Immunoblots of Vgat1 and β-actin and relative protein levels (Vgat1/β-actin) in the LPB. *$P < 0.05$, **$P < 0.01$, ***$P < 0.001$.

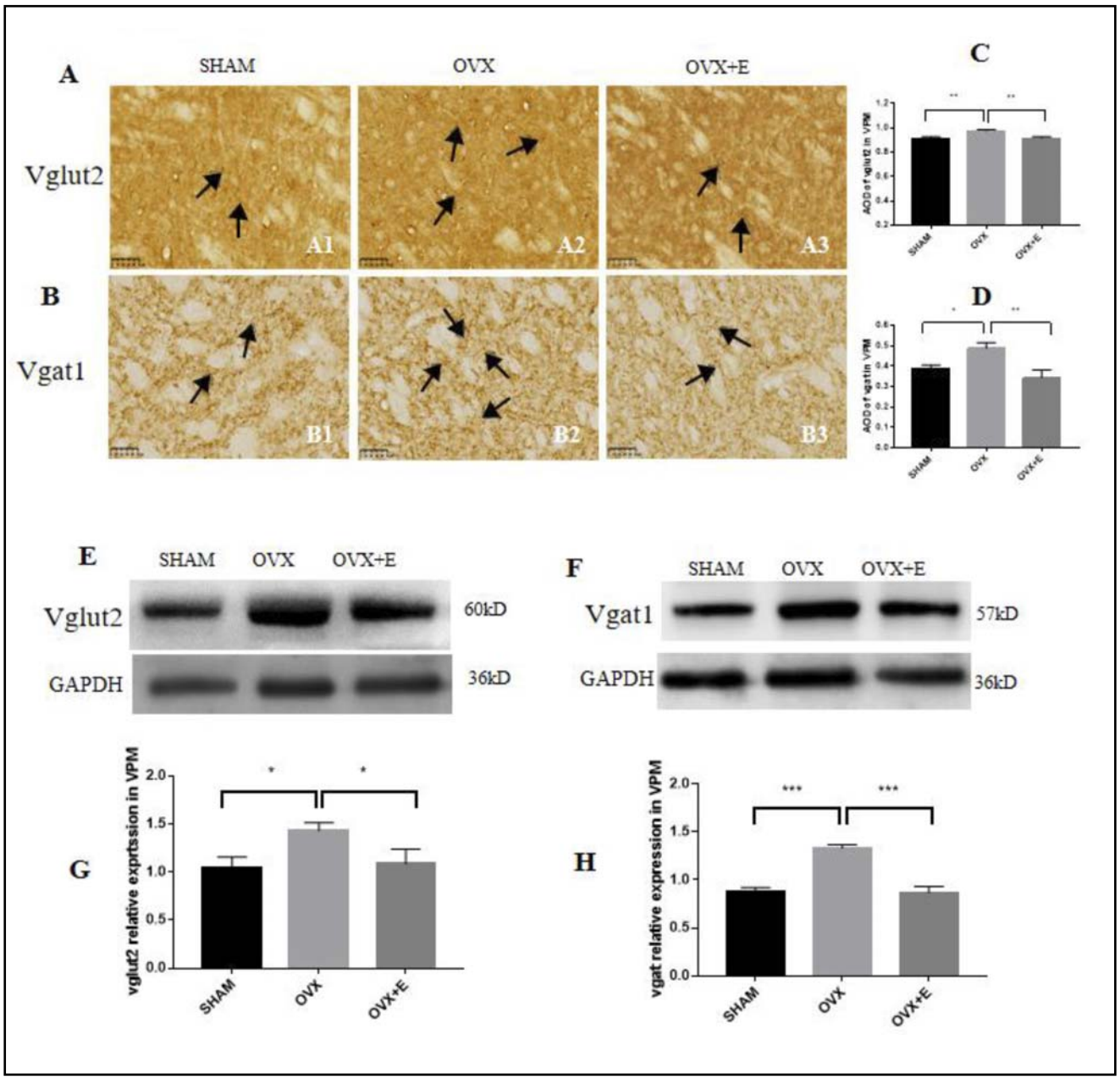

Fig. 6. (A) Immunohistochemical staining of Vglut2 in the VPM in the sham (A1), OVX (A2) and OVX+E (A3) groups. (C) Analysis of the AOD of Vglut2 in the VPM. (B) Immunohistochemical staining of Vgat1 in the VPM in the SHAM (B1), OVX (B2) and OVX+E (B3) groups. (D) Analysis of the AOD of Vgat1 in the VPM. Bar=50 μm. The arrows indicate Vglut2- and Vgat1-positive cells. (E, G) Immunoblots of Vglut2 and β-actin and relative protein levels (Vglut2/β-actin) in the VPM. (F, H) Immunoblots of Vgat1 and β-actin and relative protein levels (Vgat1/β-actin) in the VPM. **P* < 0.05, ***P* < 0.01, ****P* < 0.001.

group were significantly lower than those in the SHAM and OVX+E groups (Fig 3C, 3D; Vglut2: $P<0.05$, Vgat1: $P<0.01$). However, there was no significant difference in Vglut 2 and Vgat1 between the SHAM group and OVX+E group ($P>0.05$).

The changing trend of WB was also consistent with this finding. The gray values for Vglut2 and Vgat1 in the OVX group were significantly lower than those in the SHAM and OVX+E groups (Fig 3G, 3H; Vglut2: $P<0.01$, Vgat1: $P<0.05$). However, there was no significant difference in Vglut 2 and Vgat1 between the SHAM group and OVX+E group ($P>0.05$).

Expression of Vglut2 and Vgat1 in Sp5C

Immunohistochemistry showed that Vglut2 (Fig. 4A1-A3) and Vgat1 (Fig. 4B1-B3) were expressed in Sp5C. The AOD values for Vglut2 and Vgat1 in the OVX group were significantly lower than those in the SHAM and OVX+E groups (Fig 4C, 4D; Vglut2: $P<0.01$, Vgat1: $P<0.01$). However, there was no significant difference in Vglut 2 and Vgat1 between the SHAM group and OVX+E group ($P>0.05$).

The changing trend of WB was also consistent with this finding. The gray values for Vglut2 and Vgat1 in the OVX group were significantly lower than those in

the SHAM and OVX+E groups (Fig 4G, 4H; Vglut2: $P<0.01$, Vgat1: $P<0.01$). However, there was no significant difference in Vglut 2 and Vgat1 between the SHAM group and OVX+E group ($P>0.05$).

Expression of Vglut2 and Vgat1 in LPB

Immunohistochemistry showed that Vglut2 (Fig. 5A1-A3) and Vgat1 (Fig. 5B1-B3) were expressed in the LPB. The AOD values for Vglut2 and Vgat1 in the OVX group were significantly higher than those in the SHAM and OVX+E groups (Fig 5C, 5D; Vglut2: $P<0.01$, Vgat1: $P<0.01$). However, there was no significant difference in Vglut 2 and Vgat1 between the SHAM group and OVX+E group ($P>0.05$).

The changing trend of WB was also consistent with this finding. The gray values for Vglut2 and Vgat1 in the OVX group were significantly higher than those in the SHAM and OVX+E groups (Fig 5G, 5H; Vglut2: $P<0.05$, Vgat1: $P<0.01$). However, there was no significant difference in Vglut 2 and Vgat1 between the SHAM group and OVX+E group ($P>0.05$).

Expression of Vglut2 and Vgat1 in the VPM

Immunohistochemistry showed that Vglut2 (Fig. 6A1-A3) and Vgat1 (Fig. 6B1-B3) were expressed in the VPM. The AOD values for Vglut2 and Vgat1 in the OVX group were significantly higher than those in the SHAM and OVX+E groups (Fig 6C, 6D: Vglut2: $P<0.01$, Vgat1: $P<0.05$). However, there was no significant difference in Vglut 2 and Vgat1 between the SHAM group and OVX+E group ($P>0.05$).

The changing trend of WB was also consistent with this finding. The gray values for Vglut2 and Vgat1 in the OVX group were significantly higher than those in the SHAM and OVX+E groups (Fig 6G, 6H: Vglut2: $P<0.05$, Vgat1: $P<0.01$). However, there was no significant difference in Vglut 2 and Vgat1 between the SHAM group and OVX+E group ($P>0.05$).

DISCUSSION

The TG, as the first-level neuron of orofacial sensory information transmission, integrates peripheral afferent information and is also the key to connecting the periphery and the center. After that, the peripheral signal is transmitted to the spinal nucleus of the trigeminal nerve through the TG, and then the integrated information is transmitted to the higher center (Bičanić *et al.* 2019). Tashiro and colleagues found that high concentrations of estrogen in the rat spinal dorsal horn prevented the inhibition of GABA receptors on temporomandibular joint neurons, and this disinhibition effectively promoted the activity of GABA receptors, which effectively promoted the activity of GABA receptors, made GABA neurons play a better role and weakened the sensation of pain (Tashiro *et al.* 2014). In this study, it was found that the immunoreactivity of glutamatergic and GABAergic neurons decreased in the TG and Sp5C in ovariectomized rats, but the decrease in GABAergic neurons was greater, which showed an increase in nerve excitability. This result is consistent with that of Tashiro, suggesting that low estrogen levels have inhibitory effects on GABA and glutamatergic neurons in the TG and Sp5C but have a stronger inhibitory effect on GABA neurons so that pain signals are transmitted to the next level of neurons. The LPB, as a relay station in the orofacial sensory information transmission pathway, plays an important role in the transmission and regulation of information. The VPM is the key part of integrating all oral and facial sensory information into the cerebral cortex. In this study, it was found that the expression of glutamatergic and GABAergic neurons increased in the LPB and VPM after ovariectomy and returned to normal levels after estrogen treatment, suggesting that estrogen participates in the regulation of glutamatergic and GABAergic neurons in the LPB and VPM.

Estrogen may regulate the excitability of glutamatergic neurons through the estrogen receptor. ERα, ERβ and GPR30 receptors are expressed in the LPB and VPM (Rossetti *et al.* 2016; Warfvinge *et al.* 2020), so the effect of estrogen on glutamate and GABA neurons after ovariectomy needs to be further studied. Some studies have found that GPR30 can promote excitatory transmission by promoting the function of calmodulin-dependent protein kinase IIα (CaMKIIα) and increasing the accumulation of glutamate receptor subunit 1 (GluR1) and AMPA receptor clusters in excitatory synapses of glutamatergic neurons (Luo *et al.* 2016). In addition, some studies have found that an increase in the level of the estrogen membrane receptor GPR30 can disrupt the balance between glutamatergic and GABAergic neurons during sensory transmission in the spinal cord, resulting in an increase in pain sensation, while knocking down GPR30 can reverse this change, suggesting that estrogen and its receptors may affect the balance between these two kinds of neurons during sensory transmission (Prossnitz & Hathaway, 2015; Evrard, 2006).

In vitro experiments using hippocampal neurons have shown that an increase in estrogen levels not only leads to downregulation of GABA expression but also decreases the expression of glutamate decarboxylase (GAD), the key enzyme in the conversion of glutamate to GABA, and a decrease in GAD levels leads to a decrease in the conversion rate of glutamate to GABA, further leading to a decrease in GABA levels (Zare *et al.* 2019; Noriega *et al.* 2010). It is speculated that upon ovariectomy, the inhibitory effect of low estrogen levels on GAD was also weakened in the orofacial sensory signal transduction pathway; the increase in GAD levels led to the conversion of more glutamate to GABA, the release of glutamate decreased, and GABA immunoreactivity increased. The high estrogen level achieved after estrogen treatment restored the

inhibition of GAD expression, which led to a decrease in GABA levels.

In this study, it was found that the expression of glutamatergic and GABAergic neurons decreased in the TG and Sp5C after ovariectomy, but the decrease in inhibitory GABA neurons was higher than that in excitatory glutamatergic neurons, which made the peripheral sensory signals transmit to the center in an excitatory manner. In the LPB and VPM, the expression of these two kinds of neurons increased, the increase in excitatory glutamatergic neurons was greater than that in inhibitory GABA neurons, GABA neurons were not enough to inhibit the increased excitability of glutamatergic neurons, and sensory signals were still transmitted to the cerebral cortex, resulting in a decrease in the mechanical pain threshold. It has been confirmed that the regulation of orofacial pain is more sensitive and that estrogen is involved in the regulation of orofacial pain. In this experiment, the threshold of orofacial pain in rats was detected, and it was found that the threshold of mechanical pain decreased significantly in ovariectomized rats, which was reversed after estrogen treatment, which further confirmed this speculation. This is consistent with previous studies on the effect of estrogen on somatosensory pain. RaulSanoja *et al.* found that obvious mechanical hyperalgesia appeared in the abdomen, hindpaw and tail area of adult female ovariectomized mice. Estrogen supplementation can reverse this hyperalgesia (Sanoja & Cervero, 2008).

In this experiment, the average orofacial temperature of rats increased significantly under the condition of low estrogen. Previous studies have shown that an increase in body surface average temperature, abnormal thermoregulatory function and transient hot flushes in rats under low-estrogen conditions, which is due to the balance between glutamatergic and GABAergic neurons in the thermoregulatory pathway, which involves the LPB, is disrupted in rats, resulting in the disturbance of central thermoregulatory functions (Sun *et al.* 2020; Bansal; Aggarwal, 2019). The LPB is not only a key node in thermoregulation but also an important site for orofacial temperature signal transmission; thus, we speculate that dysregulation of the LPB leads to abnormalities not only in general thermoregulation but also in orofacial thermoregulation, leading to an increase in the temperature of the orofacial region. Thus, it is also possible that an increase in orofacial temperature can further exacerbate the mechanical sensitivity of the orofacial region.

There are some limitations in the study, as the experimental animals did not examine changes in estrogen levels but only observed the vaginal smears, uterine morphology and body weight instead. In future studies, we will test the concentration of estradiol in serum to ensure the success of ovariectomized modeling, eliminate bias and obtain more reliable results.

Summary and prospect:

Our results suggested that the equilibrium of glutamate and GABA neurons in the orofacial pain and temperature sensation pathway is broken under low-estrogen conditions, which eventually leads to a decrease in the oral and facial mechanical pain threshold and an increase in temperature. The neuroendocrine mechanism underlying the development of orofacial dysesthesia in perimenopausal women was explored in this study from a neurobiological point of view and provided related morphological evidence, providing a new theoretical basis for the identification of therapeutic targets for orofacial dysesthesia. Therefore, finding an effective way to maintain the balance of these two kinds of neurons could be a new target for the treatment of burning mouth syndrome.

REFERENCES

1 Almey A, Milner TA, Brake WG (2016). Estrogen receptor α and G-protein coupled estrogen receptor 1 are localized to GABAergic neurons in the dorsal striatum. Neurosci Lett. **622**: 118–123.
2 Bansal R, Aggarwal N (2019). Menopausal Hot Flashes: A Concise Review. J Mid-life Health. **10**: 6–13.
3 Bičanić I, Hladnik A, Džaja D, Petanjek Z (2019). THE ANATOMY OF OROFACIAL INNERVATION. Acta Clin Croat. **58**: 35–42.
4 Evrard HC (2006). Estrogen synthesis in the spinal dorsal horn: a new central mechanism for the hormonal regulation of pain. Am J Physiol-Reg I. **291**: R291–R299.
5 Herzog E, Gilchrist J, Gras C, Muzerelle A, Ravassard P, Giros B (2004). Localization of VGLUT3, the vesicular glutamate transporter type 3, in the rat brain. Neuroscience. **123**: 983–1002.
6 Hrabovszky E, Kalló I, Turi GF, May K, Wittmann G, Fekete C, et al. (2006). Expression of vesicular glutamate transporter-2 in gonadotrope and thyrotrope cells of the rat pituitary. Regulation by estrogen and thyroid hormone status. Endocrinology. **147**: 3818–25.
7 Jääskeläinen SK, Woda A (2017). Burning mouth syndrome. Cephalalgia. **37**: 627–647.
8 Kim Y, Kim HI, Kho HS (2014). Characteristics of men and premenopausal women with burning mouth symptoms: a case-control study. Headache. **54**: 888–898.
9 Kiss J, Csaba Z, Csáki A, Halász B (2013). Demonstration of estrogen receptor αprotein in glutamatergic (vesicular glutamate transporter 2 immunoreactive) neuronsof the female rat hypothalamus and amygdala using double-label immunocytochemistry. Exp Brain Res. **226**: 595–602.
10 Kuner R (2010). Central mechanisms of pathological pain. Nat Med. **16**: 1258–1266.
11 Laursen JC, Cairns BE, Dong XD, Kumar U, Somvanshi RK, Arendt-Nielsen L (2014). Glutamate dysregulation in the trigeminal ganglion: a novel mechanism for peripheral sensitization of the craniofacial region. Neuroscience. **256**: 23–35.
12 Luo J, Huang X, Li Y, Li Y, Xu X, Gao Y (2016). GPR30 disrupts the balance of GABAergic and glutamatergic transmission in the spinal cord driving to the development of bone cancer pain. Oncotarget. **7**: 73462–73472.
13 Ma Y, Liu M, Yang L, Zhang L, Guo H, Hou W (2020).Loss of Estrogen Efficacy Against Hippocampus Damage in Long-Term OVX Mice Is Related to the Reduction of Hippocampus Local Estrogen Production and Estrogen Receptor Degradation. Mol Neurobiol. **57**: 3540–3551.
14 Meurman JH, Tarkkila L, Tiitinen A (2009). The menopause and oral health. Maturitas. **63**: 56–62.
15 Micevych PE, Mermelstein PG (2008). Membrane estrogen receptors acting through metabotropic glutamate receptors: an emerging mechanism of estrogen action in brain. Mol Neurobiol. **38**: 66–77.

16 Monteleone P, Mascagni G, Giannini A, Genazzani AR, Simoncini T (2018). Symptoms of menopause - global prevalence, physiology and implications. Nat Rev Endocrinol. **14**: 199–215.
17 Moore AM, Abbott G, Mair J, Prescott M, Campbell RE (2018). Mapping GABA and glutamate inputs to gonadotrophin-releasing hormone neurones in male and female mice. J Neuroendocrinol. **30**: e12657.
18 Noriega NC, Eghlidi DH, Garyfallou VT, Kohama SG, Kryger SG, Urbanski HF (2010). Influence of 17beta-estradiol and progesterone on GABAergic gene expression in the arcuate nucleus, amygdala and hippocampus of the rhesus macaque. Brain Res. **1307**: 28–42.
19 Prossnitz ER, Hathaway HJ (2015). What have we learned about GPER function in physiology and disease from knockout mice? J Steroid Biochem. **153**: 114–126.
20 Ranjbar Ekbatan M, Cairns BE (2021). Attenuation of Sensory Transmission Through the Rat Trigeminal Ganglion by GABA Receptor Activation. Neuroscience. **471**: 80–92.
21 Reddy N, Desai MN, Schoenbrunner A, Schneeberger S, Janis JE (2021). The complex relationship between estrogen and migraines: a scoping review. Syst Rev. **10**: 72.
22 Ritchie A, Kramer JM (2018). Recent Advances in the Etiology and Treatment of Burning Mouth Syndrome. J Dent Res. **97**: 1193–1199.
23 Rossetti MF, Cambiasso MJ, Holschbach MA, Cabrera R (2016). Estrogens and Progestagens: Synthesis and Action in the Brain. J Neuroendocrinol. **28**: jne.12402
24 Sanoja R, Cervero F (2008). Estrogen modulation of ovariectomy-induced hyperalgesia in adult mice. Eur J Pain. **12**: 573–581.
25 Sears SM, Hewett SJ (2021). Influence of glutamate and GABA transport on brain excitatory/inhibitory balance. Exp Biol Med. **246**: 1069–1083.
26 Shinoda M, Kubo A, Hayashi Y, Iwata K (2019). Peripheral and Central Mechanisms of Persistent Orofacial Pain. Front Eeurosci-Switz. **13**: 1227.
27 Song IS, Ki EY, Han K, Ryu JJ, Park JB (2019). Evaluation of the Association between Menstrual Cycle Irregularity and Dental Pain or Chewing Discomfort in Women before Menopause. J Clin Med. **8**: jcm8040454.
28 Sun Y, Yang Q, Bai W, Wang W, Li Y, Luo X (2020). Changes in skin temperature of ovariectomized rats under different incubation temperatures. Geriatr Gerontol Int. **20**: 621–628.
29 Tashiro A, Bereiter DA, Thompson R, Nishida Y (2014). GABAergic influence on temporomandibular joint-responsive spinomedullary neurons depends on estrogen status. Neuroscience. **259**: 53–62.
30 Tashiro A, Nishida Y, Bereiter DA (2015). Local group I mGluR antagonists reduce TMJ-evoked activity of trigeminal subnucleus caudalis neurons in female rats. Neuroscience. **299**: 125–133.
31 Wang Z, Xu ZZ (2021). The Parabrachial Nucleus as a Key Regulator of Neuropathic Pain. Neurosci Bull. **37**: 1079–1081.
32 Warfvinge K, Krause DN, Maddahi A, Edvinsson JCA, Edvinsson L, Haanes KA (2020). Estrogen receptors α, β and GPER in the CNS and trigeminal system - molecular and functional aspects. J Headache Pain. **21**: 131.
33 Yu LH, Li N, Liu CY, Ma B (2011). Estrogen altered facial mechanical pain threshold and trigeminal P2X3 receptor expression. Neuroendocrinol Lett. **32**: 811–815.
34 Zare D, Jonaidi H, Sadeghi B (2019). Induction of hypothalamic GABA synthetic enzymes mRNA (Gad 1 and Gad 2) expression by negative energy balance in broiler and layer chicks. Neurosci Lett. **712**: 134498.
35 Zhang W, Wu H, Xu Q, Chen S, Sun L, Jiao C, et al. (2020). Estrogen modulation of pain perception with a novel 17β-estradiol pretreatment regime in ovariectomized rats. Biology of sex differences. **11**: 2.